

Publishers:

Verein Deutscher Eisenhüttenleute (VDEh)

Max-Planck-Institut für Eisenforschung GmbH

Publishing Company: Verlag Stahleisen

ISSN 0177-4832

steel research

Sonderdruck

Investigation of the orientation dependence of recovery in low-carbon steel by use of single orientation deter- mination

Dierk Raabe

Verlag Stahleisen Düsseldorf

Investigation of the orientation dependence of recovery in low-carbon steel by use of single orientation determination

Dierk Raabe

Iron poly- and oligocrystals with a carbon mass content of 0.02 % were cold rolled to a technical strain ($\varepsilon = \frac{\Delta d}{d_0}$) of 90 % and annealed at 1000 K in a salt bath furnace for 1 to 300 s. The polycrystals had an initial grain size of about 20 μm . The oligocrystals consisted of 20-40 grains with a longitudinal extension of 10-20 mm and a transverse extension of 2-6 mm. The microstructure of both types of specimens was investigated by use of optical and scanning electron microscopy. The crystallographic texture was examined by use of X-ray and electron back scattering diffraction. It is shown that both primary recrystallization and recovery considerably depend on the crystal orientation. In the 90 % cold rolled oligocrystals $\{111\}\langle uvw \rangle$ and $\{112\}\langle 110 \rangle$ oriented grains recrystallized during annealing. In crystals with $\{001\}\langle 110 \rangle$ orientation, however, primary recrystallization was suppressed. In the polycrystals the latter phenomenon was less pronounced. In these samples it was observed that $\{001\}\langle 110 \rangle$ oriented grains are consumed by growing nuclei stemming from neighbouring crystals.

Untersuchung der Orientierungsabhängigkeit der Erholung in niedriggekohltem Tiefziehstahl mit Hilfe der Einzelorientierungsbestimmung. Poly- und Oligokristalle aus Eisen mit Kohlenstoffmassenanteilen von 0.02 % wurden auf eine technische Umformung ($\varepsilon = \frac{\Delta d}{d_0}$) von 90 % kaltgewalzt und bei 1000 K in einem Salzbadofen 1-300 s lang geglüht. Die Polykristalle hatten eine Ausgangskorngröße von etwa 20 μm . Die Oligokristalle bestanden aus 20-40 Körnern mit einer Länge von 10-20 mm und einer Breite von 2-6 mm. Die Mikrostruktur beider Arten von Proben wurde mit optischer und Rasterelektronenmikroskopie, die kristallographische Textur mit Röntgen- und Elektronenbeugung im Rückstrahlverfahren untersucht. Es wird gezeigt, daß sowohl die primäre Rekristallisation als auch die Erholung stark von der Kristallorientierung abhängen. In den 90 % gewalzten Oligokristallen durchliefen Körner mit $\{111\}\langle uvw \rangle$ - und $\{112\}\langle 110 \rangle$ -Orientierungen primäre Rekristallisation im Verlauf der Glühung. In Kristallen mit $\{001\}\langle 110 \rangle$ -Orientierung jedoch wurde die primäre Rekristallisation unterdrückt. In den Polykristallen war dieses Phänomen weniger stark ausgeprägt. In diesen Proben zeigte sich, daß $\{001\}\langle 110 \rangle$ orientierte Kristalle von wachsenden Keimen aufgezehrt wurden, die der ehemaligen Korngrenze oder angrenzenden Körnern entstammten.

The mechanical properties of low carbon steels considerably depend on their microstructure and texture which are a result both of the composition of the steels and of the production methods applied. Typically, low carbon steel sheets are produced by continuous casting, slab reheating, hot rolling, hot band annealing, cold rolling and the final heat treatment. Neglecting the chemical composition and advanced processing methods like thermomechanical hot rolling or strip casting the final microstructure and texture of such steels is essentially determined by the last two processing steps. Whilst in geometrical terms cold rolling is carried out for the reduction of the sheet thickness, in physical terms it leads to the increase of the dislocation density, i.e. to the enhancement of the stored energy in the crystals. The latter fact represents a necessary prerequisite for primary recrystallization (RX). The process of RX usually takes place by the formation and movement of large angle grain boundaries. The first process is referred to as nucleation. RX thus naturally comes to an end when the grains impinge.

As was shown by various studies the mechanisms which dominate the course of RX, i.e. the kinetics and the resulting morphology, depend on numerous parameters. In case of low carbon steels among these the most relevant are the chemical composition [e.g. 1...6], the amount and type of the preceding plastic deformation [e.g. 1...6], the precipitation state [1...8] and the crystallographic texture prior to annealing [2;6;9...20]. It is well established that for the onset of RX a thermodynamic (nucleation), mechanic (net driving force vector) and kinetic (large angle grain boundary with high mobility) instability is required [1...6]. If one

of these preconditions is not fulfilled, non conservative dislocation rearrangement and mutual dislocation annihilation, viz. static recovery instead of RX prevails during annealing. Such behaviour is often observed after low degrees of deformation prior to annealing. However, it is less well established that even in case of sufficient initial cold deformation in excess of $\varepsilon = 80\%$ RX can be suppressed due to the crystallographic texture [12;13]. Owing to the mechanisms involved, during RX the texture is changed whereas during recovery it remains unchanged. Due to this principle difference it is obvious that texture investigation is an appropriate diagnostic means of distinguishing between RX and recovery. The current study is hence primarily concerned with the investigation of recovery of low carbon steel, especially with its orientation dependence, and the correlation of these observations to the deformation microstructure and texture.

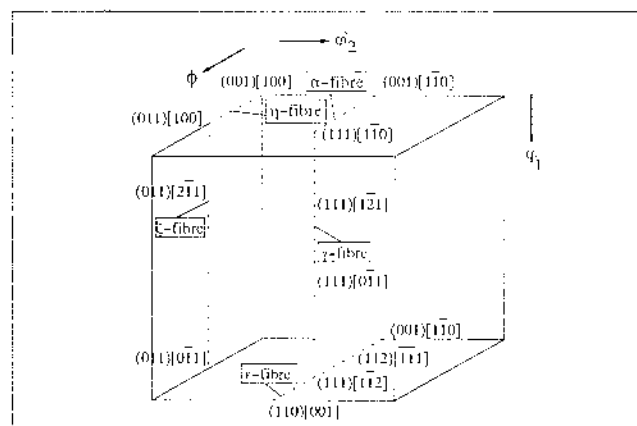


Figure 1. Some relevant crystallographic orientations of rolled and annealed ferritic steels presented in Euler space

Dr.-Ing. Dierk Raabe, group leader, Institut für Metallkunde und Metallphysik, RWTH Aachen, Germany.

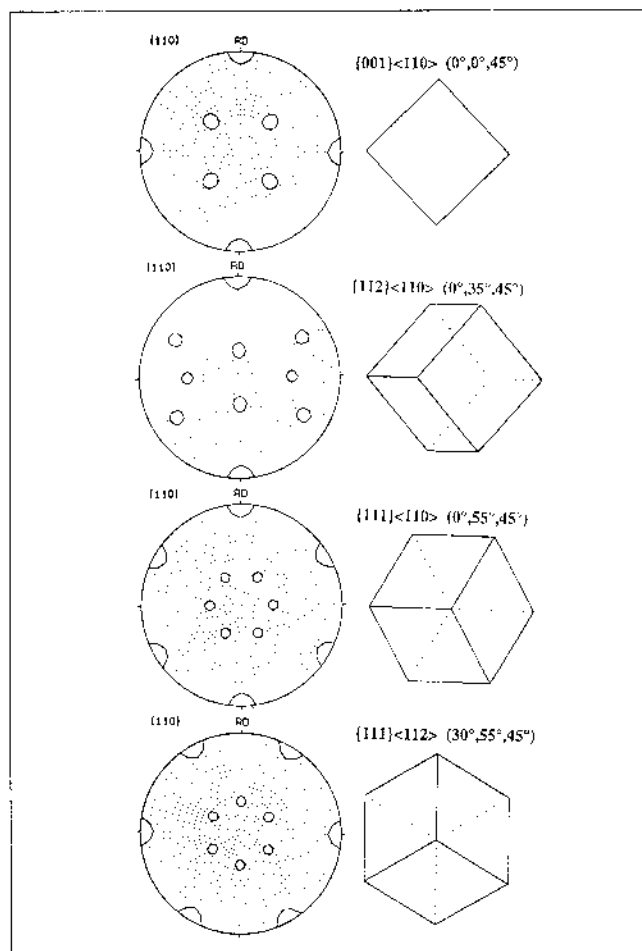


Figure 2. Some relevant crystallographic orientations of rolled and annealed ferritic steels presented in $\{110\}$ pole figures

Experimental

For the investigations poly- and oligocrystalline specimens were used. Oligocrystals are polycrystalline aggregates which consist of only a few large grains [21...23]. They were cut from directionally solidified low carbon steel. The final specimens consisted of 20-40 grains with a longitudinal extension of 10-20 mm and a transverse extension of 2-6 mm. The polycrystals had an initial grain size of about 20 μm . Both specimens contained masses of 0.02 % C.

As was shown in previous studies [21...23] oligocrystals are very convenient for examining the orientation dependent behaviour of single grains. First, the large grain size enables one to track the development of every grain during rolling [21...23] and annealing. Second, if nucleation is suppressed within a crystal, newly recrystallized grains which emerge from the initial grain boundary or adjacent crystals are usually not capable of penetrating the entire grain. This is attributed to the fact that parallel to the growth of nuclei by which the stored energy is reduced discontinuously, inside the grain the driving force is competitively reduced by recovery, i.e. continuously. If the recovering grain is large enough RX can thus come to an end before the new grains impinge. Following this argument it is hence conceivable that at the beginning of RX grains may have a stored deformation energy which suffices for producing a mechanic but not a thermodynamic or kinetic instability. However, investigating recovery only by use of oligocrystals neglects the fact that the deformation texture and microstructure, especially the degree of fragmentation and the resulting local texture gradients, are dependent on the grain size. For this reason in the present study identical experiments were carried out with poly- and oligocrystals.

Both types of samples were cold rolled to $\varepsilon = 90\%$. Subsequently the specimens were annealed at 1000 K in a salt bath furnace for 1 to 300 s. The microstructure was investigated by means of optical and scanning electron microscopy. The texture was measured using X-ray and electron diffraction. In the first case the four incomplete pole figures $\{110\}$, $\{200\}$, $\{112\}$ and $\{103\}$ were measured in the back reflection mode [24] using $\text{MoK}\alpha_1$ radiation. From the pole figures the orientation distribution function (ODF) was computed using the iterative series expansion method [25;26]. In the second case the texture was examined in grain scale making use of the orientation dependence of electron back scattering diffraction (EBSD) [27]. This technique represents a useful means of providing both, microstructure and texture data with a high spatial resolution. Details of the technique employed are explained elsewhere [28]. From every grain examined only one measured point was used for the calculation of the ODF, i.e. there is no normalization with respect to the grain size. The ODF was computed by representing each grain by a Gauss function with a scatter width of 5° in Euler space [29]. The main orientations of rolled and annealed steels are given in figures 1, 2.

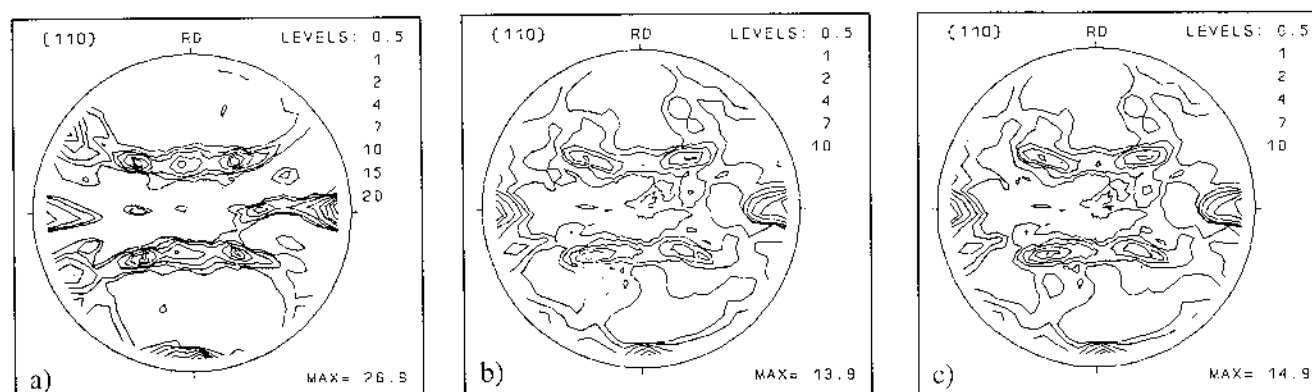


Figure 3. $\{110\}$ pole figures of a rolled and annealed oligocrystalline specimen with a strong $\{001\}\langle 110 \rangle$ rolling component; a) 90 % cold rolled, b) 90 % cold rolled and 120 s annealed (1000 K), c) 90 % cold rolled and 300 s annealed (1000 K)

Results

Oligocrystals. After 90 % cold rolling various texture components which are well known from cold rolled low carbon steels [7;9;12...20] are developed in the oligocrystals. Details of the texture evolution in oligocrystals during cold rolling were discussed elsewhere [21...23]. After rolling the specimens were annealed at 1000 K within the range 1 to 300 s. The textures which were achieved by use of X-ray diffraction, are presented in the 90 % cold rolled (a), 90 % cold rolled and 120 s annealed (1000 K) (b) and 90 % cold rolled and 300 s annealed (1000 K) (c) state in **figures 3, 5-6, 8**. Imposing longer annealing times did not lead to further texture changes. The results are arranged according to the Taylor factor of the main rolling texture component, i.e. $\{001\}\langle 110 \rangle$ grains have the lowest and $\{110\}\langle uvw \rangle$ oriented grains the largest Taylor factor. Figure 3a shows the result for a rolled sample which is characterized by a strong $\{001\}\langle 110 \rangle$ and a weak $\{111\}\langle uvw \rangle$ texture component. After annealing (figure 3b,c) the $\{001\}\langle 110 \rangle$ orientation remains entirely preserved. The initial maximum pole density of 26.9 (figure 3a) is decreased by nearly 50 % (figure 3b,c). The microstructure which corresponds to the texture shown in figure 3b is depicted in **figure 4a** (flat section, 1000 K, 120 s). Three areas with entirely different microstructures can be identified. First, an area with equiaxed newly formed grains with a size of about 15 μm (area A). Second, an area consisting of fairly equiaxed grains with a size of about 150 μm (area B). Third, an area with large, elongated, flat grains which is not recrystallized but recovered (area C). In **figure 4b** a detail of figure 4a is given together with the results which were obtained by single orientation determination. The measurements substantiate (figure 4b) that area A essentially contains $\{111\}\langle uvw \rangle$ and Goss orientations whereas area C exclusively consists of $\{001\}\langle 110 \rangle$ oriented grains.

In figure 5a a rolling texture with an incomplete α -fiber consisting of a weak $\{001\}\langle 110 \rangle$, a stronger $\{112\}\langle 110 \rangle$ and a dominating $\{111\}\langle 110 \rangle$ component is shown. During annealing all main texture components are removed (figure 5b,c). Instead, after 300 s a weak $\{111\}\langle 112 \rangle$ and an orientation close to Goss arise. The heat treatment of a specimen with a strong initial rolling component close to $\{112\}\langle 110 \rangle$ (figure 6a) leads to a considerable reduction of this orientation but not to its com-

plete elimination (figure 6a,b). As is evident from the corresponding microstructure, **figure 7**, in this sample (1000 K, 120 s) there are also areas with smaller or larger grains, respectively. However, areas containing entirely recovered grains were not found. Such regions were only detected in case that the initial rolling texture of the oligocrystal contained a strong texture maximum at $\{001\}\langle 110 \rangle$. In case of a very strong $\{111\}\langle 112 \rangle$ starting texture (figure 8a) a pronounced Goss accompanied by a weak $\{111\}\langle 110 \rangle$ component arises (figure 8b,c). In the microstructure large $\{111\}\langle 112 \rangle$ oriented grains revealed a considerable degree of fragmentation and the formation of shear bands.

Polycrystals. According to **figure 9** where the hardness of the 90 % rolled sample is shown as a function of the annealing time (1000 K) RX starts after 4 s and is completed after 10 s. First, the texture of the specimens was investigated by use of X-ray diffraction. The 90 % rolled sample revealed an incomplete α -fiber texture containing

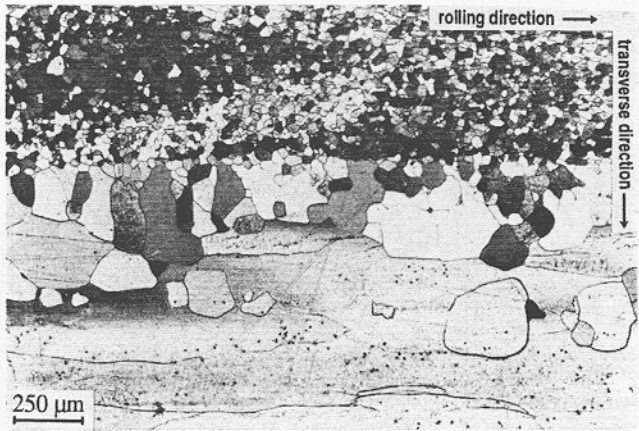


Figure 4a. Flat section of the rolled and annealed (120 s, 1000 K) oligocrystal the texture of which was shown in figure 3b

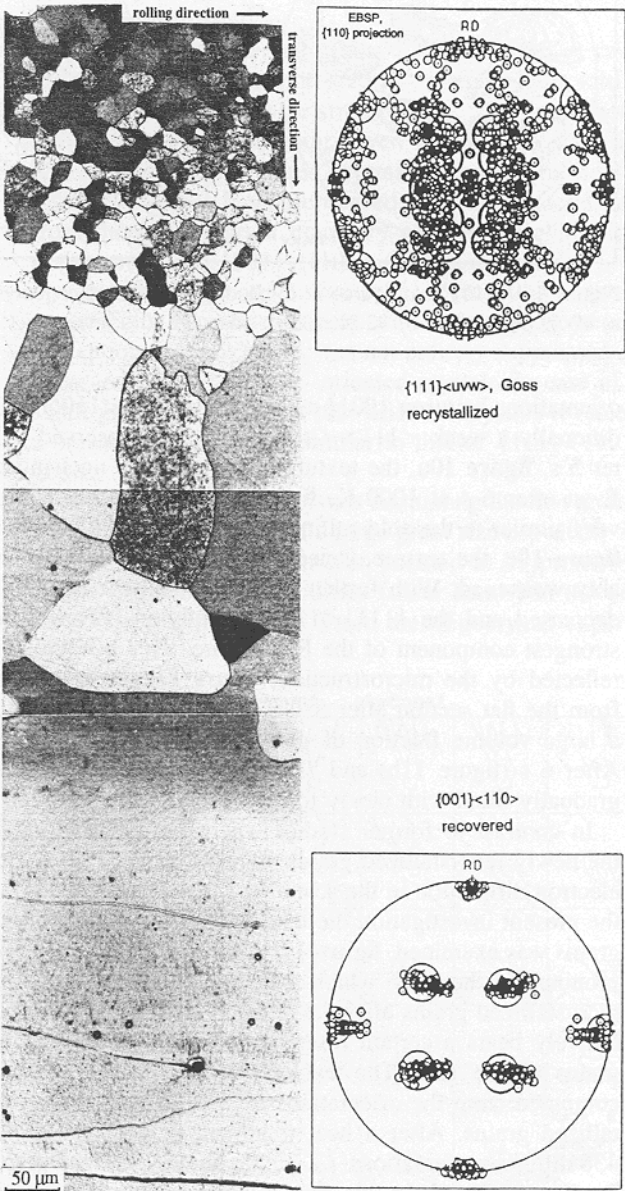


Figure 4b. Detail of the flat section presented in figure 4a together with $\{110\}$ pole figures showing the single orientations which were determined in the recrystallized and recovered area

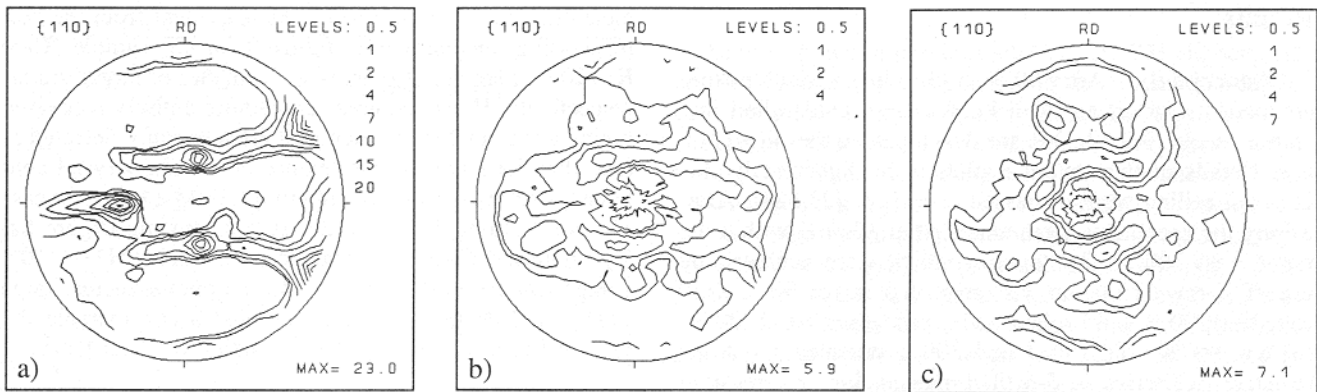


Figure 5. $\{110\}$ pole figures of a rolled and annealed oligocrystalline specimen with an incomplete α -fiber; a) 90 % cold rolled, b) 90 % cold rolled and 120 s annealed (1000 K), c) 90 % cold rolled and 300 s annealed (1000 K)

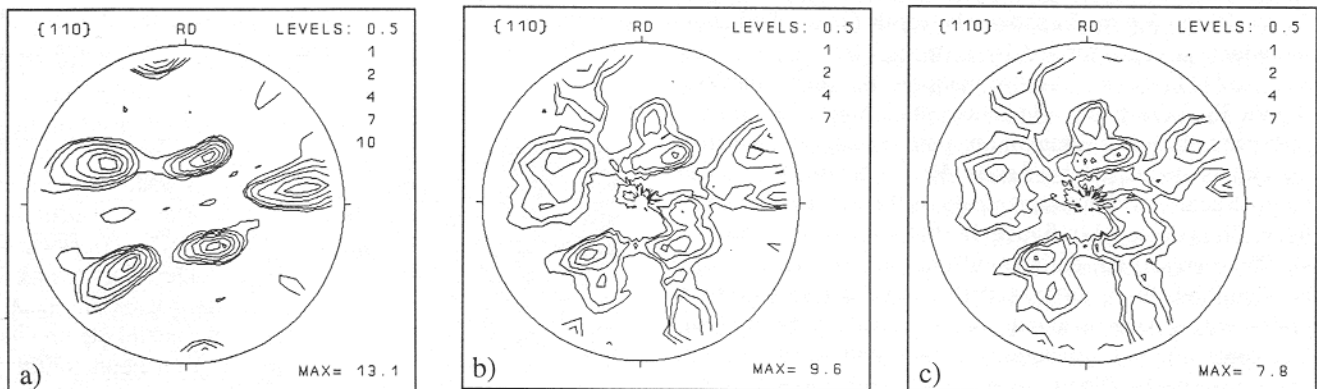


Figure 6. $\{110\}$ pole figures of a rolled and annealed oligocrystalline specimen with a strong rolling component close to $\{112\}\langle 110 \rangle$; a) 90 % cold rolled, b) 90 % cold rolled and 120 s annealed (1000 K), c) 90 % cold rolled and 300 s annealed (1000 K)

orientations between $\{001\}\langle 110 \rangle$ and $\{111\}\langle 110 \rangle$. Additionally a weak $\langle 111 \rangle \langle uvw \rangle$ fiber was observed. After 5 s, **figure 10a**, the texture appears nearly unchanged. Even after 6 s at 1000 K, **figure 10b**, the texture is still very similar to the cold rolling texture. However, after 7 s, **figure 10c**, the texture, especially the α -fiber is considerably weakened. With further heat treatment the α -fiber is decreased and the $\{111\}\langle 112 \rangle$ orientation becomes the strongest component of the RX texture. This behaviour is reflected by the microstructure, **figure 11**. As is evident from the flat section after 5 s at 1000 K (**figure 11a**) still a large volume fraction of unrecrystallized grains exists. After 6 s (**figure 11b**) and 7 s (**figure 11c**) the volume is gradually filled with newly formed grains.

In contrast to former studies where the orientations of the newly recrystallized grains were determined by use of electron diffraction in the scanning microscope [30...34] in the present investigation the texture of the unrecrystallized grains was examined, **figure 12**. Although being much less pronounced the ODF which shows the texture of the unrecrystallized grains after 5 s at 1000 K (**figure 12a**) qualitatively bears a certain resemblance to the texture of all grains (**figure 10a**). The texture shown in **figure 12a** was computed from the orientations of 781 different unrecrystallized grains. After a heat treatment of 6 s at 1000 K 438 different orientations, i.e. single unrecrystallized grains were investigated. In this case a weak texture with a pronunciation of the $\{001\}\langle 110 \rangle$ orientation is found (**figure 12b**). Most of the $\{112\}\langle 110 \rangle$, $\{111\}\langle 110 \rangle$ and $\{111\}\langle 112 \rangle$ oriented grains were hence already recrystal-

lized at this stage. The single orientation texture, however, does not bear a close resemblance to the X-ray texture (**figure 10b**). The texture which was calculated from 261 different unrecrystallized grains after 7 s at 1000 K (**figure 12c**) reveals a very strong $\{001\}\langle 110 \rangle$ component which is slightly spread out about the rolling direction. That means nearly all grains which were not yet recrystallized after 7 s had a $\{001\}\langle 110 \rangle$ orientation. In contrast, the orientation distribution which accounts for the texture of the recrystallized and the unrecrystallized grains (**figure 10c**) reveals a much lower texture characterized by a weak $\{001\}\langle 110 \rangle$, $\{111\}\langle 110 \rangle$ and $\{111\}\langle 112 \rangle$ orientation.

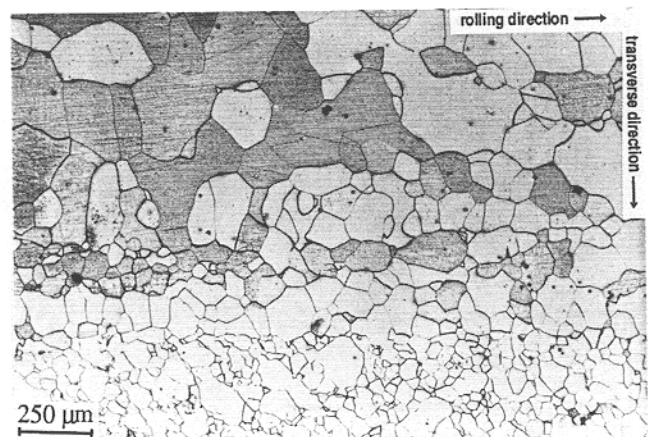


Figure 7. Flat section of the rolled and annealed (120 s, 1000 K) oligocrystal the texture of which was shown in **figure 6b**

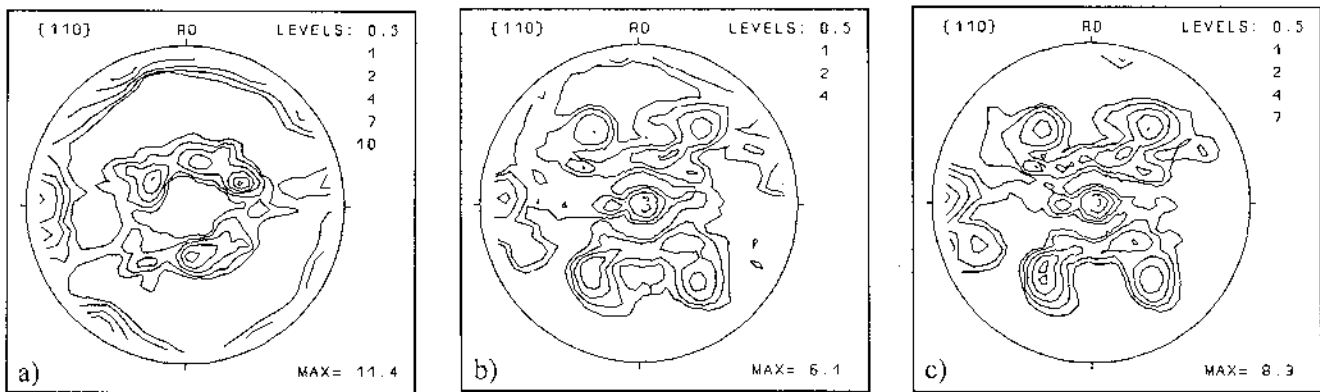


Figure 8. $\{110\}$ pole figures of a rolled and annealed oligocrystalline specimen with a strong $\{111\}\langle 112 \rangle$ rolling component; a) 90 % cold rolled, b) 90 % cold rolled and 120 s annealed (1000 K), c) 90 % cold rolled and 300 s annealed (1000 K)

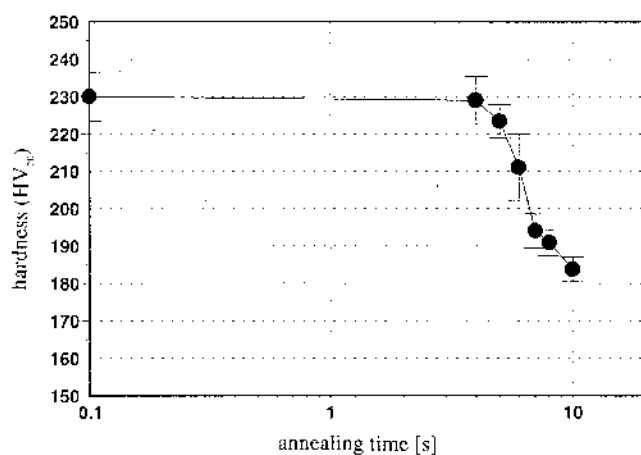


Figure 9. Hardness of the polycrystalline specimen as a function of annealing time (90 % cold rolled, 1000 K)

Discussion

From the preceding chapter the following observations, which seem to be pertinent to the discussion of recovery in low carbon steels, can be extracted:

- when studied in grain scale in both oligo- and polycrystals it becomes apparent that the kinetics of RX and the resulting grain morphology considerably depend on the initial grain orientation;
- in $\{001\}\langle 110 \rangle$ oriented grains RX is delayed in case of a small and even suppressed in case of a large initial grain size. This allows for strong recovery of grains with a $\{001\}\langle 110 \rangle$ orientation. Even at the final stage of RX $\{001\}\langle 110 \rangle$ oriented crystals do not reveal nuclei inside the grain. It was observed that nuclei stemming from the former grain boundary or from neighbouring grains grow into $\{001\}\langle 110 \rangle$ oriented crystals.
- in case of a large grain size in $\{112\}\langle 110 \rangle$ oriented grains both, RX and recovery was observed. However, nucleation in these grains was not entirely suppressed as observed in $\{001\}\langle 110 \rangle$ oriented crystals. In case of a small grain size $\{112\}\langle 110 \rangle$ oriented crystals revealed a behaviour, which was similar to that of $\{111\}\langle 110 \rangle$ grains;
- $\{111\}\langle uvw \rangle$ oriented crystals are among the first grains to recrystallize. In case of a large grain size especially in $\{111\}\langle 112 \rangle$ grains nucleation seemed to be promoted by the presence of instabilities (shear bands) in the deformation microstructure. From the oligocrystal experi-

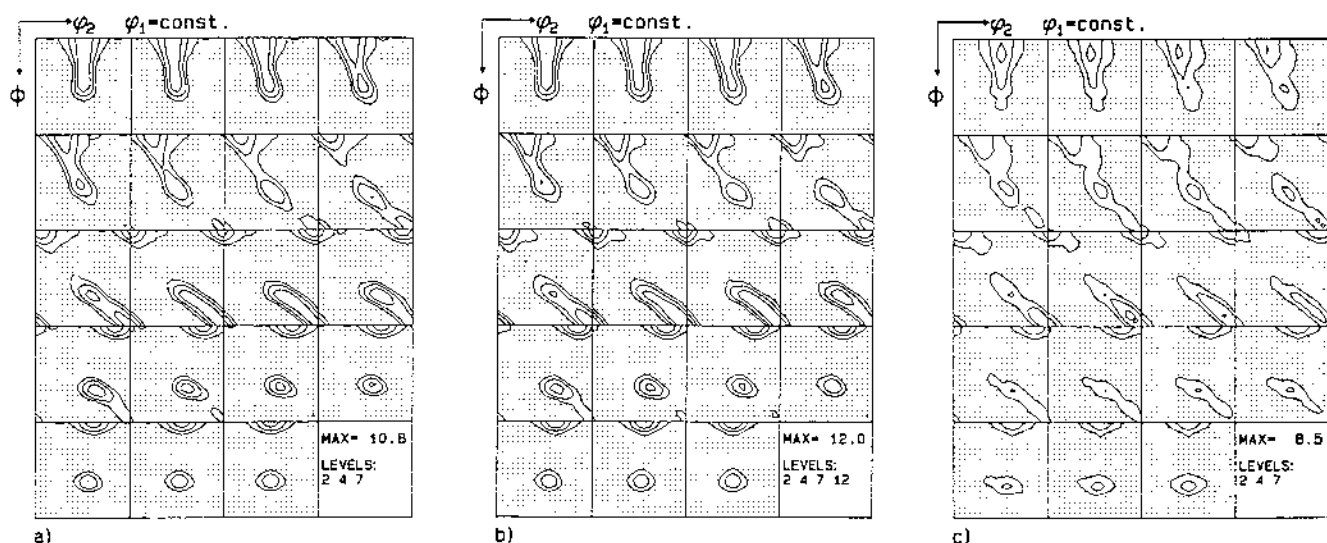


Figure 10. ODFs of the 90 % rolled and annealed polycrystals (1000 K). Incomplete pole figures measured by X-ray diffraction. Calculation of the ODF by use of the iterative series expansion method [25; 26]; a) 5 s, b) 6 s, c) 7 s at 1000 K

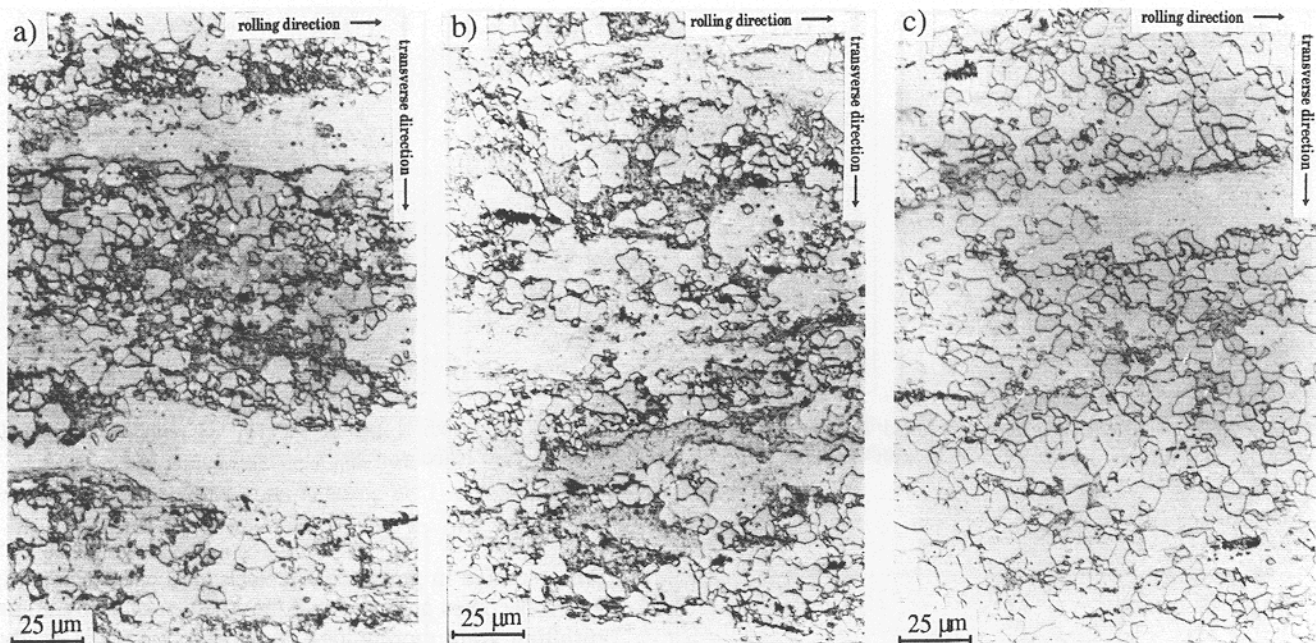


Figure 11. Flat sections of the rolled and annealed polycrystals the texture of which was shown in figure 10; a) 5 s, b) 6 s, c) 7 s at 1000 K

ments it was observed that a certain volume fraction of $\{111\}\langle 110 \rangle$ oriented crystals was generated inside $\{111\}\langle 112 \rangle$ grains and vice versa. From the difference of the macro- and microtexture of the rolled polycrystal after 6 s at 1000 K (figures 10b, 12b) it is concluded that $\{111\}\langle 110 \rangle$ is formed in the early stages of RX.

The RX behaviour of $\{111\}\langle uvw \rangle$ and $\{112\}\langle 110 \rangle$ oriented grains has already been the subject of numerous studies in the past [e.g.10...20;30...34]. In these investigations it was concluded that the tendency of $\{111\}$ grains to recrystallize can be attributed first, to the small cell sizes, i.e. to the high dislocation densities stored in them and second, to the formation of microstructural inhomogeneities such as shear bands which provide strong local misorientations within these grains. Whereas the first argument is covered by numerous studies in which transmission electron microscopy was employed [6;9;35;36] the latter fact

can be easily identified by the results shown in the present investigation (figure 8). In the oligocrystals strong shear banding occurred. Most of these bands were inclined 35° about the transverse direction. This rotation transforms the $\{111\}\langle 112 \rangle$ host orientation into the Goss component (figure 8). Although in the oligocrystals sometimes strong recovery rather than RX of $\{112\}\langle 110 \rangle$ grains was observed it is widely accepted that in fine grained polycrystals these grains are consumed due to the mechanism of growth selection [37].

Whereas the orientation dependence of RX has been widely discussed in literature, the reluctance of $\{001\}\langle 110 \rangle$ grains against RX has often been neglected, albeit it may considerably affect the microstructure and hence the properties of the final specimen. The strong orientation dependence of recovery can essentially be interpreted in two ways. The first approach is based on the assumption

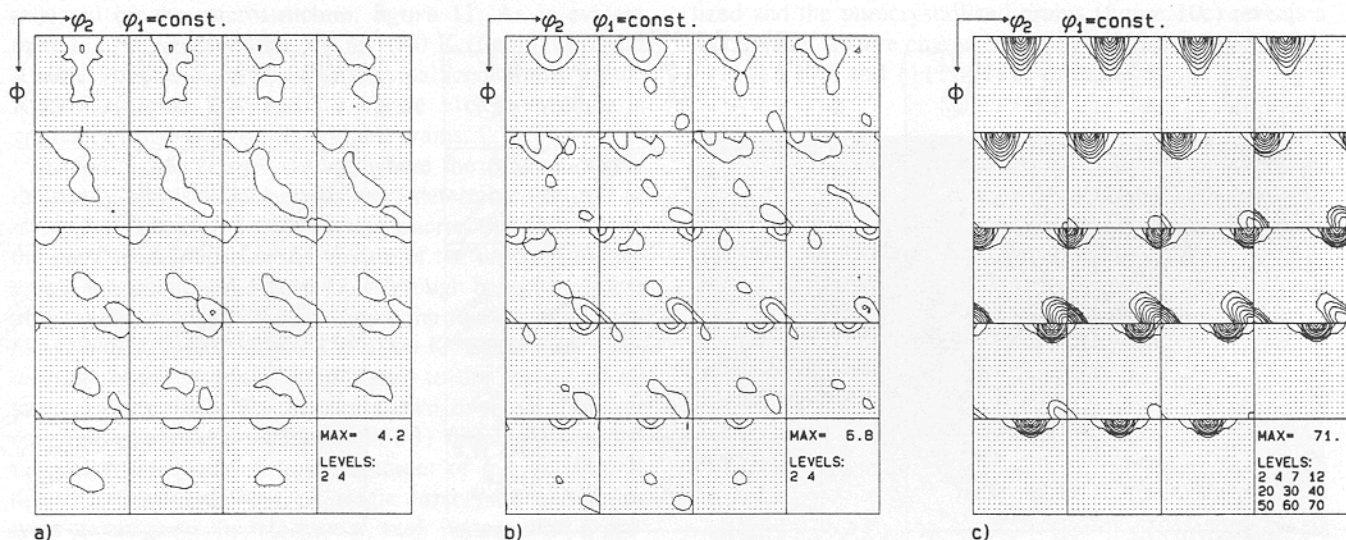


Figure 12. ODFs of the unrecrystallized grains within 90 % rolled and annealed polycrystals (1000 K). Single orientations determined by employment of electron diffraction in the scanning microscope [27;28]. Calculation of the ODF by use of the Gauss method [29]; a) 5 s, b) 6 s, c) 7 s at 1000 K

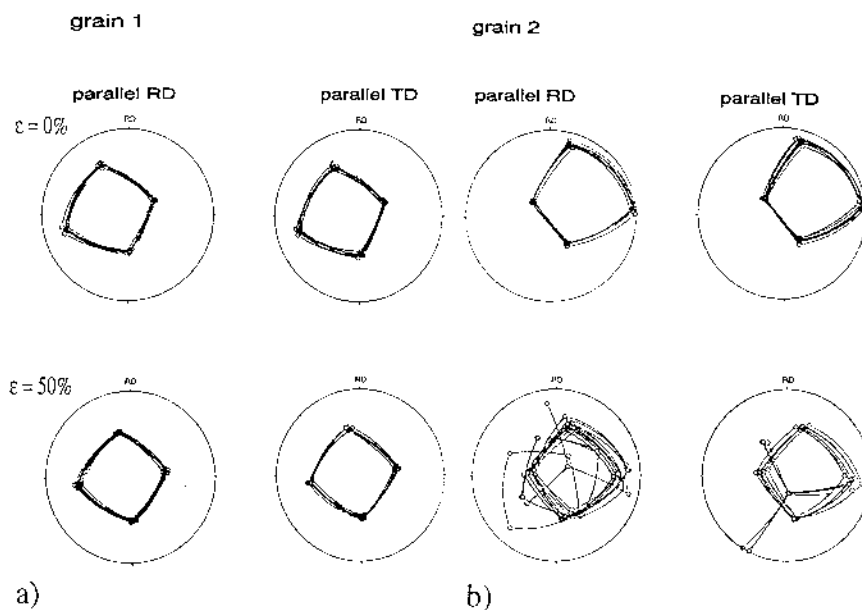


Figure 13. $\{111\}$ pole figures showing the orientation distribution within two single grains in an oligocrystalline specimen; a) grain 1: negligible local orientation gradients after 50 % rolling deformation, b) grain 2: considerable local orientation gradients after 50 % rolling deformation

that the driving force is reduced by recovery so that the mechanic instability criterion is no longer fulfilled. Recovery and RX reveal different kinetic laws. Whereas in the first case the properties change in a logarithmic manner, in the latter case an incubation period followed by a sigmoidal law is observed. It is thus conceivable that if recovery was strong enough to reduce the total driving force, i.e. the internal stress fields imposed by the stored dislocations, the movement of newly formed large angle grain boundaries would be suppressed. This assumption, however, is torpedoed by three facts. First, the energy stored in $\{001\}<110>$ oriented crystals is very low. This is suggested by numerous experimental results based on the measurement of internal stresses [35;38], stored dislocation densities and cell sizes [35;39] and related theoretical concepts such as the Taylor factor [40]. Second, recovery is not an isolated process but a preprocess to RX during which nuclei are formed. Strong recovery in the conventional sense should therefore provide a large number of nuclei rather than suppress them. Third, in case of a small grain size (polycrystals) it was observed that $\{001\}<110>$ oriented crystals are consumed by growing nuclei which proceed from the former grain boundary or even from neighbouring grains. This experience implies that $\{001\}<110>$ oriented grains provided indeed a sufficient net driving force, viz. a mechanic instability.

Consequently, the second approach for explaining the avoidance of RX is based on the assumption that albeit a mechanic instability potentially exists, the thermodynamic and kinetic instability criteria are not fulfilled in $\{001\}<110>$ oriented grains. In order to produce new large angle grain boundaries during nucleation it is essential to provide areas with large local misorientations already within the deformation microstructure. However, such orientation gradients are usually not observed within $\{001\}<110>$ oriented crystals [21...23]. This is underlined by the results shown in **figure 13**. For a large number of grains (oligocrystals) the internal orientation distribution was investigated [21...23]. The evolution of the microtexture is shown exemplary for two different single grains, one with an initial orientation close to $\{001\}<110>$ (grain 1, **figure 13a**) and one close to $\{011\}<111>$ (grain 2, **figure 13b**). Whereas after 50 % rolling deformation in grain 1 no

local misorientations occurred, grain 2 experienced considerable fragmentation. In previous studies the homogeneity of deformation of $\{001\}<110>$ oriented grains was attributed to the fact that only two slip systems are required to achieve plastic deformation even under constrained conditions. This leads to a homogeneous dislocation substructure and weak local misorientations [21...23]. In contrast, $\{111\}<uvw>$ oriented grains do not only reveal higher dislocation densities and corresponding local misorientations but also macroscopic heterogeneities like shear bands which are highly potential nucleation areas.

Following this discussion the strong recovery of $\{001\}<110>$ oriented grains has to be attributed to the suppression of RX, more precisely to the avoidance of thermodynamic and kinetic instabilities rather than to special properties of the recovery process in such grains.

Concluding remarks

Iron poly- and oligocrystals with a carbon mass content of 0.02 % were 90 % cold rolled and annealed at 1000 K for 1 to 300 s. The crystallographic texture and microstructure of both types of specimens was quantitatively investigated. By measuring the texture in grain scale it was shown that both, primary recrystallization and recovery considerably depend on the crystal orientation. In the 90 % cold rolled oligocrystals $\{111\}<uvw>$ and $\{112\}<110>$ oriented grains recrystallized during annealing. In crystals with $\{001\}<110>$ orientation, however, primary recrystallization was suppressed so that strong recovery prevailed. In the polycrystals the latter phenomenon was also observed but less pronounced. In these samples it was observed that $\{001\}<110>$ oriented grains were consumed by growing nuclei stemming from neighbouring crystals but it was rarely found that nucleation started within such grains. It was concluded that the suppression of recrystallization in $\{001\}<110>$ oriented grains has to be attributed to the avoidance of thermodynamic and kinetic instabilities.

(A 01 027; received: 03. February 1995;
in completed form: 13. February 1995)

References

- [1] *Burgers, W. G.*: Rekristallisation, verformter Zustand und Erholung, Akademische Verlagsgesellschaft, Leipzig (1941).
- [2] *Cahn, R.*: [in:] Recrystallization, Grain Growth and Textures, [ed.:] Margolin, H., ASM, Metals Park, Ohio (1966) p. 99/120.
- [3] *Haessner, F.*: [in:] Recrystallization of Metallic Materials, [ed.:] Haessner, F., Dr. Riederer Verlag GmbH Stuttgart (1984), p. 1/10.
- [4] *Lücke, K.; Stüwe, H. P.*: [in:] Recovery and Recrystallization of Metals, John Wiley and Sons, New York (1963), p. 171/92.
- [5] *Stüwe, H. P.*: [in:] Recrystallization of Metallic Materials, [ed.:] Haessner, F., Dr. Riederer Verlag GmbH Stuttgart (1984), p. 11/21.
- [6] *Doherty, R.*: [in:] Recrystallization of Metallic Materials, [ed.:] Haessner, F., Dr. Riederer Verlag GmbH Stuttgart (1984), p. 23/59.
- [7] *Raabe, D.; Lücke, K.*: Mat. Sci. Forum 157-162 (1994), p. 1033/38.
- [8] *Klinkenberg, C.; Raabe, D.; Lücke, K.*: Scr. metall. 26 (1992), p. 1137/41.
- [9] *Dillamore, I. L.; Smith, C. J. E.; Watson, T. W.*: Met. Sci. Jour. 1 (1967), p. 49/56.
- [10] *Hutchinson, W.*: Acta metall. 37 (1989), p. 1047/56.
- [11] *Hutchinson, W.*: Intern. Mat. Rev. 29 (1984), p. 25/42.
- [12] *Raabe, D.; Lücke, K.*: Mat. Sci. Forum 157-162 (1994), p. 597/610.
- [13] *Raabe, D.; Lücke, K.*: Scr. metall. 27 (1992), p. 1533/38.
- [14] *Hölscher, M.; Raabe, D.; Lücke, K.*: steel res. 62 (1991), p. 567/75.
- [15] *Wassermann, G.; Grewen, J.*: Texturen metall. Werkstoffe; 1962. Berlin-Göttingen-Heidelberg, Springer Verlag.
- [16] *Ushioda, K.; Hutchinson, W. B.; Agren, J.; Schlippenbach, U. v.*: Mat. Sci. Techn. 2 (1986), p. 807/15.
- [17] *Emren, F.; Schlippenbach, U. v.; Lücke, K.*: Acta metall. 34 (1986), p. 2105/17.
- [18] *Raabe, D.; Lücke, K.*: Mater. Sci. Techn. 9 (1993), p. 302/12.
- [19] *Inokuti, Y.; Doherty, R.*: Acta metall. 26 (1978), p. 61/80.
- [20] *Inagaki, H.*: Z. Metallkunde 82 (1991), p. 265/74.
- [21] *Boeslau, J.; Raabe, D.*: Mater. Sci. Forum 157-162 (1994), p. 501/06.
- [22] *Raabe, D.*: Phys. stat. sol. 181b (1994), p. 291/99.
- [23] *Raabe, D.; Boeslau, J.*: Proc. 15th Riso Int. Symp. on Mat. Science: Numeri. Pred. of Def. Proc. and the Behaviour of Real Materials, [eds.:] S.L. Andersen, J.B. BildeSorensen, T. Lorentzen, O.B. Pedersen and N.J. Sorensen. RISO Nat. Lab, Roskilde, Denmark (1994), p. 481/86.
- [24] *Schulz, L. G.*: Journ. Appl. Phys. 20 (1949), p. 1030/35.
- [25] *Bunge, H. J.; Esling, C. J.*: Physique - Lettr. 40 (1979), p. 627/31.
- [26] *Dahms, M.; Bunge, H. J.*: J. Appl. Cryst. 22 (1989), p. 439/47.
- [27] *Venables, J.; Harland, C.*: Philos. mag. 27 (1973), p. 1193/1200.
- [28] *Engler, O.; Gottstein, G.*: steel res. 63 (1992), p. 413/18.
- [29] *Lücke, K.; Pospiech, J.; Virmich, K. H.; Jura, J.*: Acta metall. 29 (1981), p. 167/85.
- [30] *Böttcher, A.; Hastenrath, M.; Hjelen, J.; Lücke, K.*: Scr. metall. 27 (1992), p. 1115/20.
- [31] *Lindh, E.; Hutchinson, B.; Bate, P.*: Mat. Sci. Forum 157-162 (1994), p. 997/1002.
- [32] *Böttcher, A.*: Zur Bildung der Goss Textur in RGO - Elektroblech, Aachen. 1990 (Dr.-Ing. thesis).
- [33] *Plutka, B.*: Untersuchungen zu Vorgängen bei der Bildung von Rekristallisationstexturen in Tiefziehstählen, Aachen, 1991 (Dr.-Ing. thesis).
- [34] *Raabe, D.*: Texturen kubisch-raumzentrierter Übergangsmetalle, Aachen. 1992 (Dr.-Ing. thesis).
- [35] *Dillamore, I. L.; Morris, P. L.; Smith, C. J. E.; Hutchinson, W. B.*: Proc. Roy. Soc. 329A (1972), p. 405/14.
- [36] *Swann, P.; Nutting, J.*: Journ. Inst. Met. 90 (1961), p. 133/45.
- [37] *Ihe, G.; Lücke, K.*: Arch. Eisenhüttenwes. 39 (1968), p. 693/98.
- [38] *Lebrun, J. L.; Maeder, G.; Parniere, P.*: Proc. 5th Int. Conf. on Textures of Materials Bd. 2, Springer Verlag, [eds.:] Gottstein, G.; Lücke, K. (1978), p. 513/18.
- [39] *Smith, C.; Dillamore, I. L.*: Metal Sci. 8 (1974), p. 73/80.
- [40] *Taylor, G. I.*: Journ. Inst. Met. 62 (1938), p. 307/12.